University of Nebraska - Lincoln

DigitalCommons@University of Nebraska - Lincoln

Nitrogen loss from soil through anaerobic ammonium oxidation coupled to iron reduction

Wendy H. Yang
University of California, Berkeley, wendy_yang@berkeley.edu

Karrie A. Weber
University of Nebraska-Lincoln, kweber@unl.edu

Whendee L. Silver
University of California, Berkeley, wsilver@berkeley.edu

Nitrogen loss from soil through anaerobic ammonium oxidation coupled to iron reduction

Wendy H. Yang,[1] Karrie A.Weber,[2] and Whendee L. Silver [1]

1. Department of Environmental Science, Policy, and Management, University of California, Berkeley, California 94720
2. School of Biological Sciences and Department of Earth and Atmospheric Sciences, University of Nebraska-Lincoln, Lincoln, Nebraska 68588

Corresponding author — W. H. Yang, email wendy_yang@berkeley.edu

Abstract

The oxidation of ammonium is a key step in the nitrogen cycle, regulating the production of nitrate, nitrous oxide and dinitrogen. In marine and freshwater ecosystems, anaerobic ammonium oxidation coupled to nitrite reduction, termed anammox, accounts for up to 67% of dinitrogen production.[1–3] Dinitrogen production through anaerobic ammonium oxidation has not been observed in terrestrial ecosystems, but the anaerobic oxidation of ammonium to nitrite has been observed in wetland soils under iron-reducing conditions.[4, 5] Here, we incubate tropical upland soil slurries with isotopically labelled ammonium and iron(iii) to assess the potential for anaerobic ammonium oxidation coupled to iron(iii) reduction, otherwise known as Feammox,[6] in these soils. We show that Feammox can produce dinitrogen, nitrite or nitrate in tropical upland soils. Direct dinitrogen production was the dominant Feammox pathway, short-circuiting the nitrogen cycle and resulting in ecosystem nitrogen losses. Rates were comparable to aerobic nitrification[7,8] and to denitrification,[9] the latter being the only other process known to produce dinitrogen in terrestrial ecosystems. We suggest that Feammox could fuel nitrogen losses in ecosystems rich in poorly crystalline iron minerals, with low or fluctuating redox conditions.

Terrestrial net primary productivity is often limited by the availability of fixed nitrogen (N) owing in large part to the mobility of N across ecosystem boundaries, particularly through denitrification.[10] Denitrification is dominantly a microbial process that converts nitrate (NO_3^-) to nitrous oxide (N_2O) and dinitrogen (N_2) gases. In terrestrial ecosystems, denitrification is thought to be the only process by which fixed N is converted to N_2, thereby completing the nitrogen cycle. In aquatic systems, anammox bypasses the potential for N_2O production as well as decreasing internal N cycling. Bacteria capable of anammox have been detected in soil,[11, 12] but the occurrence of anammox has not been demonstrated in terrestrial ecosystems.[13]

The reduction of ferric iron (Fe(iii)) can be coupled to anaerobic ammonium (NH_4^+) oxidation to produce N_2 (reference 14), NO_3^- (reference 14), or NO_2^- (references 4–6). This process is termed Feammox[6] and theoretically could occur abiotically or be microbially mediated. There is some evidence of Feammox to NO_2^- in wetland soils,[4, 5] but Feammox to N_2 has not been previously described nor has Feammox been measured in upland soils. Feammox to N_2 is energetically more favorable than Feammox to NO_2^- or NO_3^- and is favorable over a wider range of conditions. Environments rich in poorly crystalline Fe minerals, such as highly weathered soils, have the potential to support Feammox. Under conditions typically found in soil,

Feammox to N_2 using ferrihydrite, a common poorly crystalline Fe oxide, yields $-245 \, kJ \, mol^{-1}$ reaction (see Supplementary Equations) through the following process (equation (1)):

$$3Fe(OH)_3 + 5H^+ + NH_4^+ \rightarrow 3Fe^{2+} + 9H_2O + 0.5N_2 \qquad (1)$$
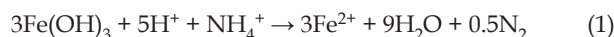
This reaction remains energetically favorable over a wide pH range. Feammox to NO_2^- (equation (2)) occurs only below pH 6.5, stoichiometrically requires more Fe(iii) and yields less energy than Feammox to N_2 ($-164 \, kJ \, mol^{-1}$ reaction) under the same conditions:

$$6Fe(OH)_3 + 10H^+ + NH_4^+ \rightarrow 6Fe^{2+} + 16H_2O + NO_2^- \qquad (2)$$
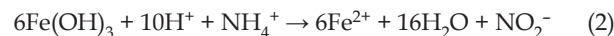
Feammox to NO_3^- is also thermodynamically feasible under these conditions ($-207 \, kJ \, mol^{-1}$ reaction).

Feammox rates averaged $1.20 \pm 0.28 \, \mu g \, N \, g^{-1} \, d^{-1}$ (±standard error of the mean) following the addition of both $^{15}NH_4^+$ and Fe(iii) to a tropical forest soil (Figure 1a). These rates are conservative estimates determined from $^{30}N_2$ production alone and are comparable to gross aerobic nitrification rates in tropical forests.[7, 8, 15] Lower $^{30}N_2$ production occurred following the addition of $^{15}NH_4^+$ alone ($0.32 \pm 0.13 \, \mu g \, N \, g^{-1} d^{-1}$, $p < 0.001$), presumably resulting from the utilization of background Fe in the Feammox reaction. These soils are rich in poorly crystalline, reactive Fe ($6.2 \pm 0.2 \, mg \, Fe \, g^{-1}$ soil[16]); thus, sufficient background Fe(iii) was available to drive $^{30}N_2$ production with the addition of $^{15}NH_4^+$ alone. At 24 h after $^{15}NH_4^+$ addition, HCl-extractable Fe(iii) concentrations averaged $528 \pm 128 \, \mu g \, Fe(iii) \, g^{-1}$. We used replicate ($n=8$) upland soils (0–10 cm depth) from the Luquillo Mountains, Puerto Rico, USA. Soils were slurried and pre-incubated in an anaerobic glove box to remove O_2, inhibit aerobic nitrification, and deplete background NO_2^- and NO_3^-. Rigorous procedures were used to exclude molecular O_2 from the experiment, thereby removing the possibility of aerobic nitrification (see Supplementary Discussion). We then measured $^{30}N_2$ ($^{30}N_2 = {}^{15}N + {}^{15}N$) and $^{29}N_2$ ($^{29}N_2 = {}^{15}N + {}^{14}N$) mole fractions of headspace gas in samples and soil-free jars (that is, blanks) to determine $^{30}N_2$ and $^{29}N_2$ production rates (see Supplementary Methods). Feammox directly to N_2 or Feammox-generated NO_2^- followed by denitrification or anammox are the only possible sources of $^{30}N_2$ (Table 1). At least two possible mechanisms exist for Feammox: surface Fe reduction coupled to NH_4^+ oxidation, or O_2 liberated from Fe oxides used for intra-aerobic NH_4^+ oxidation coupled to Fe reduction, similar to anaerobic methane oxidation coupled to NO_2^- reduction carried out by oxygenic bacteria.[17]

Figure 1. Mean $^{30}N_2$ and $^{29}N_2$ production rates. a) Mean $^{30}N_2$ production rates following the addition of $^{15}NH_4^+$, $^{15}NH_4^+$+Fe(iii) or $^{15}NH_4^+$+Fe(iii) + C_2H_2. The addition of Fe(iii) and Fe(iii) +C_2H_2 significantly increased mass $^{30}N_2$ relative to $^{15}NH_4^+$ alone ($p < 0.001$, $p = 0.08$, respectively). **b)** Mean $^{29}N_2$ production rates following the addition of $^{15}NH_4^+$ or $^{15}NH_4^+$+Fe(iii) ($p = 0.02$). Error bars represent standard errors ($n = 8$).
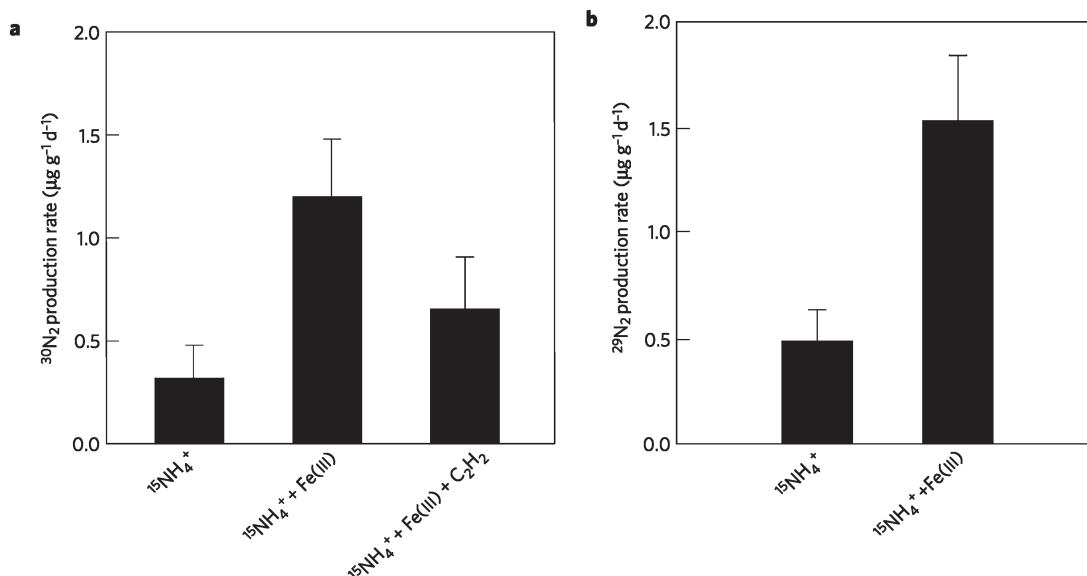
Table 1. Potential pathways for $^{30}N_2$ and $^{29}N_2$ production from $^{15}NH_4^+$ under anoxic conditions.*

Product	Nitrogen substrate 1	Nitrogen substrate 2	Process
$^{30}N_2$	Added $^{15}NH_4^+$	Added $^{15}NH_4^+$	Feammox to N_2
	Added $^{15}NH_4^+$	Feammox-generated $^{15}NO_2^-/^{15}NO_3^{-\dagger}$	Anammox
	Feammox-generated $^{15}NO_2^-/^{15}NO_3^-$	Feammox-generated $^{15}NO_2^-/^{15}NO_3^-$	Denitrification
$^{29}N_2$	Added $^{15}NH_4^+$	Background $^{14}NH_4^+$	Feammox to N_2
	Added $^{15}NH_4^+$	Background $^{14}NO_2^-/^{14}NO_3^-$	Anammox
	Feammox-generated $^{15}NO_2^-/^{15}NO_3^-$	Background $^{14}NH_4^+$	Anammox
	Feammox-generated $^{15}NO_2^-/^{15}NO_3^-$	Background $^{14}NO_2^-/^{14}NO_3^-$	Denitrification

* Dissimilatory NO_3^- reduction to NH_4^+ cycles background $^{14}NO_2^-/^{14}NO_3^-$ or Feammox-generated $^{15}NO_2^-/^{15}NO_3^-$ to $^{14}NH_4^+$ or $^{15}NH_4^+$, respectively. Thus, it does not create additional pathways for $^{30}N_2$ and $^{29}N_2$ production from $^{15}NH_4^+$.
† Feammox can generate $^{15}NO_2^-$ or $^{15}NO_3^-$ from added $^{15}NH_4^+$

Feammox directly to N_2 accounted for 47 (±27) to 72 (±9)% of $^{30}N_2$ loss in the Fe(iii) and $^{15}NH_4^+$ treatment (see Supplementary Methods). We used acetylene (C_2H_2) to separate direct N_2 production through Feammox from gaseous N loss through denitrification of Feammox-generated NO_2^- and NO_3^-. Acetylene blocks the reduction of N_2O to N_2 (reference 18), allowing N_2O produced from denitrification to accumulate in the headspace. The presence of C_2H_2 decreased $^{30}N_2$ production ($p = 0.08$; Figure 1a), indicating that 53±27% of $^{30}N_2$ loss resulted from Feammox to NO_2^- or NO_3^-. The rate of Feammox to NO_2^- or NO_3^- estimated from the difference in $^{30}N_2$ production with and without C_2H_2 addition was $0.59±0.32 \mu g\,N\,g^{-1}\,d^{-1}$. Based on N_2O production rates in the presence of C_2H_2, approximately $0.33 ± 0.08 \mu g\,N\,g^{-1}\,d^{-1}$ was oxidized to NO_2^- or NO_3^- and then subsequently reduced to N_2O through denitrification (28±9% of $^{30}N_2$ production). These two separate estimates suggest that Feammox directly to N_2 dominates as the gaseous N loss pathway.

We also measured significant $^{29}N_2$ production following the addition of $^{15}NH_4^+$ alone ($p = 0.03$) and following the addition of Fe(iii) and $^{15}NH_4^+$ together ($p < 0.001$; Figure 1b). The production rate of $^{29}N_2$ was significantly greater following Fe(iii) and $^{15}NH_4^+$ addition compared with $^{15}NH_4^+$ addition alone ($p = 0.02$). Overall, $^{29}N_2$ accounted for 60±12% of the total $^{15}N-N_2$ produced, which is consistent with the value of 66% predicted from random combinations of background $^{14}NH_4^+$ and added $^{15}NH_4^+$. The production of $^{29}N_2$ is interesting for several reasons. First, the proportion of $^{29}N_2$ produced

suggests that there was not preferential utilization of added $^{15}NH_4^+$ for N_2 production during the experiment, indicating that the $^{14}NH_4^+$ and $^{15}NH_4^+$ pools were well mixed. Second, there are several potential sources of $^{29}N_2$ including Feammox to NO_2^- followed by anammox to N_2, the use of background $^{14}NH_4^+$ along with added $^{15}NH_4^+$ in Feammox to N_2, or a combination of pathways involving Feammox-generated NO_2^- or NO_3^- followed by denitrification (Table 1). All of these pathways, however, require anaerobic NH_4^+ oxidation. Third, the stimulation of $^{29}N_2$ with Fe(iii) addition further indicates that Feammox played an important role in anaerobic NH_4^+ oxidation, regardless of the ultimate mechanism for $^{29}N_2$ generation. Considering the production of both $^{30}N_2$ and $^{29}N_2$, anaerobic NH_4^+ oxidation consumed 5–14% of the added $^{15}NH_4^+$ label during the experiment.

In a time-series experiment $^{30}N_2$ production occurred rapidly, within 1.5h of adding $^{15}NH_4^+$ and Fe(iii) (Figure 2). The change in $^{30}N_2$ mole fraction over 1.5h was equivalent to Feammox rates of $0.48 ± 0.11 \mu g\,N\,g^{-1}\,d^{-1}$. Feammox rates were relatively constant over 9 h and averaged $0.11 ± 0.01 \mu g\,N\,g^{-1}\,d^{-1}$. These rates were lower than in the previous experiment, probably owing to the higher pH of the soil (pH5.21±0.28 relative to 4.27±0.02). Theoretically Feammox rates will decrease as pH increases because the reaction becomes less thermodynamically favorable and the reactivity of Fe oxide minerals decreases as pH increases.[19] To test this we conducted a third experiment in tropical forest soils with an initial pH of 6.12±0.03. The rate of $^{30}N_2$ production following $^{15}NH_4^+$ and Fe(iii) addition was

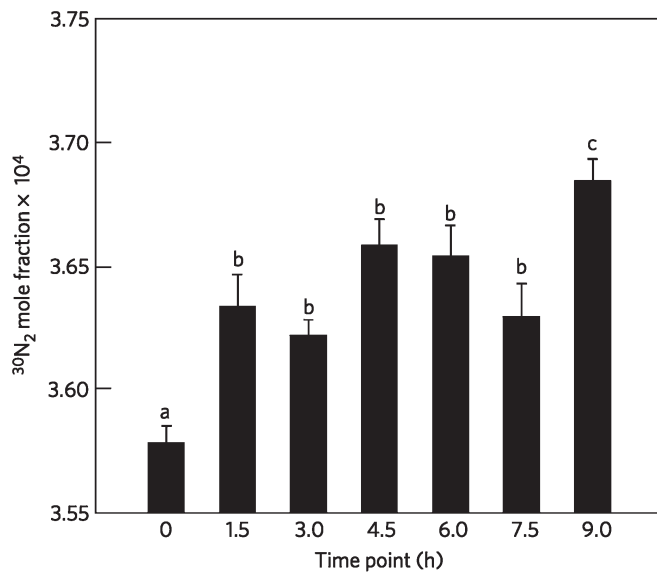**Figure 2. Change in mean $^{30}N_2$ mole fraction over 9 h.** Mean $^{30}N_2$ mole fraction following the addition of $^{15}NH_4^+$+Fe(iii) in the time-series experiment. Lowercase letters indicate statistically significant differences among time points using a repeated measures analysis of variance ($p < 0.05$). Bars are mean values ($n = 8$) and standard errors.

Figure 3: Mean $^{30}N_2$ production rate at pH 6. Mean $^{30}N_2$ production rates following the addition of $^{15}NH_4^+$ or $^{15}NH_4^+$+Fe(iii) to tropical forest soils above pH 6. Error bars represent standard errors ($n = 8$). n.d. = not detectable within a detection limit of $0.007\,\mu g\,^{15}N\,g^{-1}\,d^{-1}$. There was no statistically significant increase in $^{30}N_2$ production with Fe(iii) addition.

considerably lower than under more acidic conditions ($0.02 \pm 0.01\,\mu g\,N\,g^{-1}\,d^{-1}$ during the first 6 h) and did not vary significantly at 12 or 25 h (Figure 3). Iron reduction increased by $115 \pm 67\,\mu g$ Fe(iii) $g^{-1}\,d^{-1}$ with NH_4^+ and Fe(iii) addition compared with NH_4^+ addition alone, approximately reflecting the 140 µg Fe g^{-1} of Fe(iii) added. This suggests that the added Fe(iii) was readily reducible, although only a small proportion of the Fe(iii) reduced was likely to be associated with NH_4^+ oxidation (see Supplementary Methods).

In a series of calculations, we estimate a potential Feammox rate of $1–4\,kg\;NH_4^+–N\,ha^{-1}\,y^{-1}$ (0–10 cm depth). Incubations with added substrate may have stimulated Feammox under laboratory conditions and thus we used the theoretical ratios of 3–6 moles of Fe(iii) reduced per mole of NH_4^+ oxidized based on the thermodynamic calculations instead of measured laboratory rates. Using this approach, only 0.4–0.8% of Fe reduction is attributable to Feammox. We assumed a mean Fe reduction rate of $25\,\mu g\,Fe\,g^{-1}\,d^{-1}$ after weighting Fe reduction by the temporal O_2 dynamics previously measured at the field site.[20] This rate of Fe reduction is considerably lower than those measured in the anaerobic slurries, which may have also been stimulated under laboratory conditions (see Supplementary Methods). These results suggest that Feammox is roughly equivalent to total denitrification estimated for this forest.[9] Similar to denitrification and aerobic nitrification, Feammox is likely to be highly variable in space and time owing to spatial and temporal heterogeneity in substrate availability, redox potential, and pH.

Feammox provides alternative loss pathways of N from soils, decreasing N_2O emissions if NH_4^+ is oxidized directly to N_2, or potentially increasing N_2O emissions if Feammox results in NO_2^- or NO_3^- followed by incomplete denitrification. However, here we indicate that Feammox to N_2 is the dominant gaseous N loss pathway. Our estimates here have considered Feammox only in the top 10 cm of soil, but NH_4^+, Fe(iii) and reducing conditions also occur deeper in the soil profile, increasing the importance of this NH_4^+ oxidation pathway.
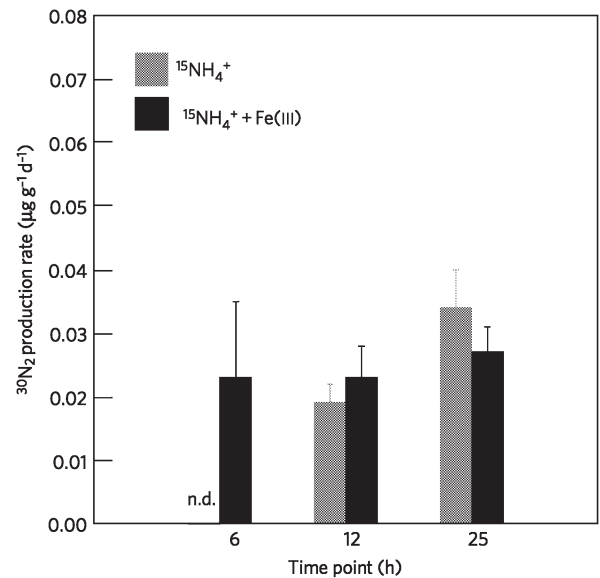
Feammox is likely to occur in Fe-rich soils that experience periods of anoxia or contain anoxic microsites. Frequent low-redox events have been measured in upland soils in humid regions, during periods of rainfall, or when O_2 consumption exceeds diffusive resupply.[20-24] Even in well-drained soils, high rates of Fe reduction can occur in well-aggregated clay and organic colloids.[25] Feammox has not been considered in ecosystem or global models of N cycling and could change our estimates of total N losses from terrestrial environments.

Methods

We slurried surface soil (0–10 cm depth) from the Luquillo Experimental Forest. Fresh soil was collected for each experiment on different dates at different locations and was transported to the University of California within 24 h at ambient temperature in gas-permeable bags. Large roots, leaves, worms and rocks were removed by hand. The fresh soil was then slurried in a 3:1 ratio of milliliters of deionized water (DIW) to grams of soil (oven-dry equivalent). Slurry aliquots, 110 g each, were divided into 240 ml jars. We also prepared blank jars containing 100 ml DIW. The slurries and blank jars were pre-incubated in the dark in an anaerobic glove box for six days to deplete pre-existing O_2, NO_2^-, and NO_3^-. Each experiment was entirely carried out in an anaerobic glove box (Coy Laboratory Products) equipped with palladium catalyst packs to remove O_2 and a gas analyzer to monitor O_2 concentrations, which remained at 0 ppm throughout the experiments. The glove-box headspace composition was approximately 90% N_2, 8% carbon dioxide (CO_2), and 2% hydrogen.

We carried out a series of three experiments. In the first experiment, we incubated soil with the following treatments to determine if Feammox occurs in soils and to identify the relative importance of the Feammox pathways: $^{15}NH_4^+$ addition; $^{15}NH_4^+$ and Fe(iii) addition; $^{15}NH_4^+$, Fe(iii), and C_2H_2 addition; and soil-free jars (blanks) containing DIW ($n = 8$ per treatment). We sampled the jar headspace gas after 24 h of incubation. In the second experiment, we determined the timescale at which Feammox occurs after the addition of $^{15}NH_4^+$ and Fe(iii) ($n = 8$). We sampled headspace gas from the same jars at 1.5 h intervals up to 9 h after NH_4^+ and Fe(iii) addition. We calculated $^{30}N_2$ production rates for each sample from the linear change in $^{30}N_2$ mole fraction between two given time points. In the third experiment, we measured

Feammox rates in soil at higher pH (≥ 6) to determine the effect of pH on Feammox rates. We incubated soil slurries with the following three treatments: $^{15}NH_4^+$ addition, $^{15}NH_4^+$ and Fe(iii) addition, and soil-free blank jars containing DIW ($n = 8$ per treatment). We sampled the jar headspace gas for determination of $^{30}N_2$ mole fraction at 6, 12, and 25 h of incubation. In each experiment we added $6 \mu g N–^{15}NH_4Cl\,g^{-1}$ and sufficient Fe(iii) to drive Feammox to NO_2^- using a stoichiometric molar ratio of 6:1 Fe(iii) to $^{15}NH_4^+$. The amount of $^{15}NH_4^+$ added was chosen to increase our ability to detect changes in $^{29}N_2$ and $^{30}N_2$ mole fractions while keeping the NH_4^+ pool size at a realistic level. Ammonium pools typically range from 1 to $15 \mu g N\,g^{-1}$ in this tropical forest and are not correlated with O_2 availability.[7, 8, 26]

At each sampling time point, each jar was shaken vigorously to equilibrate the N_2 between dissolved and gas phases. Duplicate gas samples were taken with gas-tight $500 \mu l$ syringes equipped with zero-volume stopcocks and immediately analyzed for isotopic composition for $^{29}N_2$ and $^{30}N_2$ mole fraction. A detailed description of the $^{15}N_2$ gas analysis technique is given in the Supplementary Methods. A third gas sample (50 ml) was stored for analysis of N_2O concentration on a Shimadzu GC-14A equipped with an electron capture detector.

After the final gas sampling, the slurries were subsampled for pH measurement using a pH electrode (Denver Instruments) and then extracted in 2 M KCl for colorimetric analysis of NH_4^+ and NO_3^- using an autoanalyzer (Lachat Quik Chem flow injection analyzer, Lachat Instruments). The extracts were shaken with phosphate and filtered to remove Fe that could interfere with colorimetric NO_3^- analysis.[27] In the third experiment, we also used a 0.5 N HCl extraction to determine acid-extractable Fe(ii) concentration. Owing to the high Fe(ii) concentrations in the extracts, we used a modified ferrozine method[25] to quantify Fe(ii) concentrations on a Genesys 20 spectrophotometer (ThermoFisher). Iron reduction rates were calculated from the linear change in Fe(ii) concentrations between sampling time points. All extractions were carried out in the anoxic glove box.

We calculated $^{15}N–NH_4^+$ oxidation rates from the difference in jar headspace $^{29}N_2$ or $^{30}N_2$ mole fractions between samples and soil-free blanks (where $^{29}N_2$ or $^{30}N_2$ mole fraction = moles of $^{29}N_2$ or $^{30}N_2$ divided by moles of total N_2). To determine $^{15}N–NH_4^+$ oxidation rates from $^{15}N_2$ production, we used the stoichiometry of the Feammox to N_2 pathway. We determined the proportion of Feammox directly to $^{30}N_2$ as the difference between Feammox to $^{30}N_2$ and Feammox to NO_2^- and/or NO_3^-. A detailed description of the methods is given in the Supplementary Information.

References

1. Dalsgaard, T. & Thamdrup, B. Factors controlling anaerobic ammonium oxidation with nitrite in marine sediments. *Appl. Environ. Microbiol.* 68, 3802–3808 (2002).
2. Kuypers, M. M. M. *et al*. Massive nitrogen loss from the Benguela upwelling system through anaerobic ammonium oxidation. *Proc. Natl Acad. Sci. USA* 102, 6478–6483 (2005).
3. Schubert, C. J. *et al*. Anaerobic ammonium oxidation in a tropical freshwater system (Lake Tanganyika). *Environ. Microbiol.* 8, 1857–1863 (2006).
4. Clement, J. C., Shrestha, J., Ehrenfeld, J. G. & Jaffe, P. R. Ammonium oxidation coupled to dissimilatory reduction of iron under anaerobic conditions in wetland soils. *Soil Biol. Biochem.* 37, 2323–2328 (2005).
5. Shrestha, J., Rich, J., Ehrenfeld, J. & Jaffe, P. Oxidation of ammonium to nitrite under iron-reducing conditions in wetland soils: Laboratory, field demonstrations, and push-pull rate determination. *Soil Sci.* 174, 156–164 (2009).
6. Sawayama, S. Possibility of anoxic ferric ammonium oxidation. *J. Biosci. Bioeng.* 101, 70–72 (2006).
7. Silver, W. L., Herman, D. J. & Firestone, M. K. Dissimilatory nitrate reduction to ammonium in upland tropical forest soils. *Ecology* 82, 2410–2416 (2001).
8. Templer, P., Silver, W. L., Pett-Ridge, J., DeAngelis, D. & Firestone, M. K. Plant and microbial controls on nitrogen retention and loss in a humid tropical forest. *Ecology* 89, 3030–3040 (2008).
9. Chestnut, T., Zarin, D., McDowell, W. & Keller, M. A nitrogen budget for late-successional hillslope tabonuco forest, Puerto Rico. *Biogeochemistry* 46, 85–108 (1999).
10. Vitousek, P. M. & Howarth, R. W. Nitrogen limitation on land and in the sea: How can it occur. *Biogeochemistry* 13, 87–115 (1991).
11. Penton, C., Devol, A. & Tiedje, J. Molecular evidence for the broad distribution of anaerobic ammonium-oxidizing bacteria in freshwater and marine sediments. *Appl. Environ. Microbiol.* 72, 6829–6832 (2006).
12. Humbert, S. *et al*. Molecular detection of anammox bacteria in terrestrial ecosystems: Distribution and diversity. *ISME J.* 4, 450–454 (2010).
13. Jetten, M. *et al*. Biochemistry and molecular biology of anammox bacteria. *Crit. Rev. Biochem. Mol. Biol.* 4, 65–84 (2009).
14. Luther, G. W., Sundby, B., Lewis, B. L., Brendel, P. J. & Silverberg, N. Interactions of manganese with the nitrogen cycle: Alternative pathways to dinitrogen. *Geochim. Cosmochim. Acta* 61, 4043–4052 (1997).
15. Davidson, E. A. *et al*. Processes regulating soil emissions of NO and N_2O in a seasonally dry tropical forest. *Ecology* 74, 130–139 (1993).
16. Dubinsky, E. A., Silver, W. L. & Firestone, M. K. Tropical forest soil microbial communities couple iron and carbon biogeochemistry. *Ecology* 91, 2604–2612 (2010).
17. Ettwig, K. F. *et al*. Nitrite-driven anaerobic methane oxidation by oxygenic bacteria. *Nature* 464, 543–547 (2010).
18. Yoshinari, T., Hynes, R. & Knowles, R. Acetylene inhibition of nitrous oxide reduction and measurement of denitrification and nitrogen fixation in soil. *Soil Biol. Biochem.* 9, 177–183 (1977).
19. Cornell, R. M. & Schwertmann, U. *The Iron Oxides: Structure, Properties, Reactions, Occurrences, and Uses* (Wiley, 2003).
20. Liptzin, D., Silver, W. L. & Detto, M. Temporal dynamics in soil oxygen and greenhouse gases in two humid tropical forests. *Ecosystems* 14, 171–182 (2011).
21. Sexstone, A. J., Revsbech, N. P., Parkin, T. B. & Tiedje, J. M. Direct measurement of oxygen profiles and denitrification rates in soil aggregates. *Soil Sci. Soc. Am. J.* 49, 645–651 (1985).
22. Faulkner, S. P. & Faulkner, W. H. Redox processes and diagnostic wetland soil indicators in bottomland hardwood forests. *Soil Sci. Soc. Am. J.* 56, 856–865 (1992).
23. Silver, W. L., Lugo, A. E. & Keller, M. Soil oxygen availability and biogeochemistry along rainfall and topographic gradients in upland wet tropical forest soils. *Biogeochemistry* 44, 301–328 (1999).
24. Schuur, E. A. G. & Matson, P. A. Net primary productivity and nutrient cycling across a mesic to wet precipitation gradient in Hawaiian montane forest. *Oecologia* 128, 431–442 (2001).
25. Liptzin, D. & Silver, W. L. Effects of carbon addition on iron reduction and phosphorus availability in a humid tropical forest soil. *Soil Biol. Biochem.* 41, 1696–1702 (2009).
26. Pett-Ridge, J., Silver, W. L. & Firestone, M. K. Redox fluctuations frame microbial community impacts on N-cycling rates in a humid tropical forest soil. *Biogeochemistry* 81, 95–110 (2006).
27. Yang, W. H., Herman, D. J., Liptzin, D. & Silver, W. L. A new approach for removing iron interference from soil nitrate analysis. *Soil Biol. Biochem.* 46, 123–128 (2012).

Supplementary Information follows.

Nitrogen loss from soil through anaerobic ammonium oxidation coupled to iron reduction

Wendy H. Yang[1], Karrie A. Weber[2], and Whendee L. Silver[1]

1. Department of Environmental Science, Policy, and Management, University of California, Berkeley, CA 94720, USA.

2. School of Biological Sciences and School of Earth and Atmospheric Sciences, University of Nebraska-Lincoln. Lincoln, NE, 68588, USA.

Supplementary Information

1. Supplementary Methods

Study Site

Surface soil (0-10 cm depth) was collected from the Bisley Research Watersheds in the Luquillo Experimental Forest, Puerto Rico. Soils are deep and highly weathered, derived from volcanoclastic material and classified as Ultisols and Oxisols[28]. The climate is relatively aseasonal with a mean annual temperature of 19.1° C and a mean annual precipitation of 3500 mm[29-30].

Experimental Treatment Additions

The $^{15}NH_4^+$, Fe(III), and DI solutions were prepared anoxically[31], sealed in serum bottles with an anoxic N_2 gas headspace, and stored in the glove box before use. The

Fe(III) was added as hydrous ferric oxide (HFO) synthesized from ferric chloride hexahydrate[32]. Background NH_4^+ concentrations were measured after the pre-incubation period during the first (5.25 ± 0.13 µg N g^{-1}, $^{15}NH_4^+$ enrichment to 54 atom %) and third experiments (11.05 ± 0.21 µg N g^{-1}; $^{15}NH_4^+$ pool enrichment to 38 atom %). In the first experiment, background $NO_3^- + NO_2^-$ concentrations after anoxic pre-incubation averaged 1.30 ± 0.44 µg N g^{-1}, and in the third experiment, background $NO_3^- + NO_2^-$ concentrations averaged 0.70 ± 0.23 µg N g^{-1}. This presence of $NO_3^- + NO_2^-$ after anoxic pre-incubation may be due to background NO_3^- and/or NO_2^- production via Feammox.

For the first experiment, the jars were sealed immediately after the treatment solutions were pipetted into the anoxically pre-incubated slurries with custom-made viton gaskets and aluminum lids equipped with 1/8" Swagelok o-seal fittings and septa for gas sampling. For the second and third experiments, the slurry jars were sealed 24 hours before the treatment solutions were injected into the jars. For all experiments, the jars remained sealed until after the last gas sampling. To begin the incubations, 1 mL of each treatment solution was added. For the $^{15}NH_4^+$ only treatment, 1 mL DI was added in lieu of the Fe(III) solution. For the C_2H_2 treatment, 50 mL headspace gas was removed and replaced with 50 mL C_2H_2 to achieve 30 % C_2H_2 in the headspace. Previous tests showed that lower concentrations of C_2H_2 did not completely inhibit N_2O reduction. The C_2H_2 was generated from calcium carbide and de-gassed DI inside of a pre-evacuated vial that had been flushed with helium three times. All jars were shaken vigorously to distribute the treatment solutions and dissolve the C_2H_2.

Gas Analysis

For the first experiment, 100 µL gas samples were immediately analyzed for $^{15}N_2$ on a PDZ Europa isotope ratio mass spectrometer (IRMS) by direct injection from the gas-tight syringes. The sample was injected upstream of a heated copper reduction tube, Carbosorb trap, and magnesium perchlorate trap to remove O_2, CO_2, and water vapor online. For subsequent experiments, 400 µL gas samples were analyzed on an IsoPrime 100 IRMS (Elementar, Hanau, Germany) interfaced with a custom-built $^{15}N_2$ gas analysis system that uses gas chromatography, cryotrapping, and other online gas purification to remove O_2, nitric oxide, carbon monoxide, and other gases that can cause interference in measurements of *m/z* 28, 29, and 30. Ultra-high purity N_2 was used as a standard that was periodically analyzed throughout the day to account for instrument drift. The standard deviation of the references over the course of one day was 10^{-6} for the $^{29}N_2$ mole fraction and 10^{-5} for the $^{30}N_2$ mole fraction on the Europa system and $5 * 10^{-7}$ for the $^{29}N_2$ mole fraction and $3 * 10^{-6}$ for the $^{30}N_2$ mole fraction on the IsoPrime system. Stored gas samples were analyzed for N_2O concentration on a Shimadzu GC-14A equipped with an ECD.

Statistical Analyses

We performed all statistical analyses using SYSTAT Version 10 (SPSS Inc., Evanston, IL). We log-transformed data as needed to meet the assumptions of student's t-tests. We performed two-tailed student's t-tests to compare $^{29}N_2$ and $^{30}N_2$ mole fractions between treatments and blanks to determine if significant NH_4^+ oxidation occurred for a

given treatment. We also compared $^{30}N_2$ or $^{29}N_2$ production rates between treatments

using two-tailed student's t-tests. We used Gaussian error propagation to estimate errors

in rates of Feammox to NO_2^- or NO_3^- as well as errors in the percentage of $^{30}N_2$ loss

attributed to direct Feammox to N_2.

Calculation of Nitrogen Transformation Rates

We calculated ^{15}N-NH_4^+ oxidation rates from the difference in jar headspace $^{29}N_2$ or $^{30}N_2$

mole fractions between samples and soil-free blanks (where $^{29}N_2$ or $^{30}N_2$ mole fraction =

moles of $^{29}N_2$ or $^{30}N_2$ divided by moles of total N_2). We calculated the moles of

headspace $^{29}N_2$ or $^{30}N_2$ by multiplying the $^{29}N_2$ or $^{30}N_2$ mole fractions by the moles of

total headspace N_2. We determined the moles of total headspace N_2 in the jars by using

the ideal gas law. The atmospheric pressure was assumed to be 1 atm, and the air

temperature was maintained at 24° C throughout the experiments. The jar headspace

volume was calculated from the empty jar volume (240 mL) and the weight of the slurry,

which was 75 % water (density, 1 g cm^{-3}) and 25 % dry soil equivalent (bulk density,

0.63 g cm$^{-3[33]}$). The background air in the glove box was approximately 90 % N_2, and we

assumed that the N_2 concentration did not change detectably during the incubation.

Sensitivity analyses show that a 5 % error in the assumed N_2 concentration translates into

a 5 % error in the calculated NH_4^+ oxidation rates.

To determine ^{15}N-NH_4^+ oxidation rates from $^{15}N_2$ production, we used the

stoichiometry of the Feammox to N_2 pathway (equation 1), which states that 2 moles of

NH_4^+ are required to produce one mole of N_2. We accounted for the fact that only one N

atom in $^{29}N_2$ is ^{15}N-labeled whereas both N atoms in $^{30}N_2$ are ^{15}N-labeled. The NH_4^+

oxidation rates were expressed per gram of oven dry soil equivalent in each jar. For our

lab experiments, we conservatively report the oxidation of $^{15}NH_4^+$ as Feammox or

anaerobic NH_4^+ oxidation rates rather than scale the $^{15}NH_4^+$ oxidation rates to the ^{15}N-

enrichment of the NH_4^+ pools to obtain total rates that include oxidation of both $^{14}NH_4^+$

and $^{15}NH_4^+$.

We determined the proportion of Feammox directly to $^{30}N_2$ as the difference

between Feammox to $^{30}N_2$ and Feammox to NO_2^- and/or NO_3^- calculated using the two

approaches outlined below. First, we took the difference between measured rates of

Feammox to $^{30}N_2$ without and with C_2H_2, which inhibits the reduction of N_2O to N_2. This

calculation is based on the assumptions that the N_2O produced was derived from the

$^{15}NO_2^-$ and/or $^{15}NO_3^-$ generated by Feammox and that the $^{15}N_2O$ was denitrified to $^{30}N_2$

without C_2H_2. The first assumption was supported by the accumulation of N_2O in the

headspace in the presence of C_2H_2 and the absence of O_2, ruling out aerobic nitrification.

The latter assumption was supported by the lack of N_2O accumulation in the chamber

headspace in the absence of C_2H_2. For a second, independent approach, we calculated

theoretical NH_4^+ oxidation rates from N_2O production in the presence of C_2H_2 (no N_2O

accumulated in the absence of C_2H_2). Nitrous oxide production rates were calculated

using the Henry's law constant to account for production of both gas and dissolved

phases of N_2O. We used the stoichiometry of the Feammox to NO_2^- pathway (equation

2), which states that 1 mole of NH_4^+ is required to produce 1 mole of NO_2^-. We then

assumed that 2 moles of NO_2^- were required to produce 1 mole of N_2O via denitrification.

The high concentration of C_2H_2 required to completely inhibit N_2O reduction (30 %) precludes $^{15}N_2O$ isotopic analysis[34]; thus, this approach could have overestimated Feammox to $^{15}N_2O^-$ or $^{15}NO_3^-$ by including ^{14}N-N_2O production via Feammox.

Calculation of Ecosystem Feammox Rate

To determine the proportion of Fe reduction that was associated with Feammox, we conservatively used conditions from the $^{15}NH_4^+$ addition treatment of the third experiment at pH 6, which exhibited the lowest Feammox rates. The average Fe(III) reduction rate was 232 ± 50 μg Fe(III) g^{-1} d^{-1}, well within the range reported for humid tropical forest soils (approximately 3-800 ug Fe(III) g^{-1} d^{-1}[16, 25, 35-38]. The percentage of Fe(III) reduction attributed to Feammox was 0.4 ± 0.1 % given a theoretical ratio of 3 moles of Fe(III) reduced per mole of NH_4^+ oxidation to N_2^- (equation 1) or 0.8 ± 0.2 % given a theoretical ratio of 6 moles of Fe(III) reduced per mole of NH_4^+ oxidation to NO_2^- or NO_3^- (equation 2) based on thermodynamic calculations.

We weighted Fe reduction rates by temporal O_2 dynamics in the field to better represent the potential periods when Feammox was favorable. We used the frequency distribution of bulk soil O_2 concentrations (at 10 cm depth) previously measured at our study site. Bulk soil O_2 concentrations were < 1 % for 20 % of the time and > 1 % for 80 % of the time[21]. Fe reduction rates previously measured in intact soil from this study site incubated under 21 % O_2 averaged 2.7 μg Fe(III) g^{-1} d^{-1}[28], and we used this value to represent Fe reduction rates under aerobic conditions. Fe reduction rates measured in slurried soils under anoxic conditions for the third Feammox experiment averaged $232 \pm$

50 μg Fe(III) g^{-1} d^{-1}. In a pilot experiment, we observed Fe reduction rates that were twice as high in slurried soils compared to intact soils that were placed in an anoxic glove box for 23 h. We therefore assumed that the Fe reduction rate for intact soil under anoxic conditions was half that for slurried soils, 116 μg Fe(III) g^{-1} d^{-1}. Thus, the overall Fe reduction rate weighted for temporal O$_2$ dynamics was 25 μg Fe(III) g^{-1} d^{-1}.

If 0.4 - 0.8 % of Fe reduction (0.1 - 0.2 μg Fe(III) g^{-1} d^{-1}) in the top 10 cm of soil is associated with Feammox and soil bulk density is 0.63 g cm^{-3}[33], then on the ecosystem scale, Feammox rates are approximately 1 - 4 kg NH$_4^+$ oxidized ha^{-1} y^{-1}, comparable to total denitrification estimated for this forest[8].

2. Supplementary Discussion

We took multiple precautions to remove molecular O$_2$ from the soil slurries and thus prevent the contribution of aerobic nitrification to NH$_4^+$ oxidation. We note that our procedures were similar to or more rigorous than those typically used for quantification of anammox[1-3]. The experiments were performed entirely inside an anaerobic glove box which was maintained at O$_2$ concentrations below 1 ppm (the detection limit of the gas analyzer). In addition, dissolved O$_2$ concentrations in the soil slurries were monitored during the pre-incubation period using a ProODO optical dissolved O$_2$ sensor (YSI, Yellow Springs, OH). Dissolved O$_2$ concentrations were below the instrument detection limit of 1 μM within 24 hours of pre-incubation. Treatment solutions were prepared anoxically[31] and accounted for a 2.4 % increase in the water volume of the soil slurries so that negligible O$_2$ was introduced with the treatment solutions.

Here we outline a calculation to demonstrate that the amount of O_2 needed to account for the observed NH_4^+ oxidation rates is much greater than was present given the measurements of glove box headspace O_2 concentration as well as dissolved O_2 concentrations in the soil slurries. Feammox rates averaged 1.20 µg N g^{-1} dry soil d^{-1} with NH_4^+ and Fe(III) addition in soils at pH 4.2. This is equivalent to 0.4 mg N-$^{15}NH_4^+$ L^{-1} water d^{-1} in the soil slurries with a 3:1 gravimetric ratio of water to dry soil. Over a 24 h incubation, 0.4 mg N-$^{15}NH_4^+$ L^{-1} or 27 µmol N-$^{15}NH_4^+$ L^{-1} was oxidized. The stoichiometric ratio of O_2:NH_4^+ consumed during aerobic nitrification is 1.5:1, and as such, 41 µM O_2 would be needed to account for the observed NH_4^+ oxidation rates. Dissolved O_2 concentrations in the soil slurries were < 1 µM within 24 h of pre-incubation, and the slurries were pre-incubated for 6 days total with the last day in sealed jars (for the second and third experiments). Thus, there was insufficient O_2 present in the jars for aerobic nitrification to account for the measured Feammox rates.

The difference in $^{30}N_2$ production with and without C_2H_2 could be interpreted as reflecting the inhibition of aerobic nitrification. Given the calculation above, 20 µM O_2 would be required for aerobic nitrification to account for the 0.59 µg N g^{-1} dry soil d^{-1} difference in $^{30}N_2$ production rates with and without C_2H_2. Thus, the difference in $^{30}N_2$ production with and without C_2H_2 represents only the contribution of Feammox to NO_2^- or NO_3^- to total Feammox rates.

3. Supplementary Equations

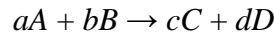## Calculation of the Thermodynamic Favorability of Feammox Reactions

The change in Gibbs free energy was calculated to determine thermodynamic favorability of balanced Feammox reactions using the following equation:

$$\Delta G_r = \Delta G_r^{\circ} + RT \ln \frac{\{C\}^c \{D\}^d}{\{A\}^a \{B\}^b}$$
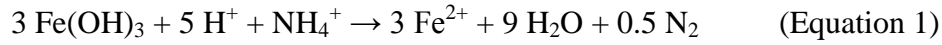
Where:

$$\Delta G_r^{\circ} = c\Delta G_{fD}^{\circ} + d\Delta G_{fD}^{\circ} - a\Delta G_{fA}^{\circ} - b\Delta G_{fB}^{\circ}$$

For the generalized reaction:

$$aA + bB \rightarrow cC + dD$$

The energy yield of the balanced redox reaction is denoted as ΔG_r, whereas ΔG_r° is the sum of the free energy of formation for a chemical species multiplied by the number of moles of each of the products, minus the sum of the free energy of formation multiplied by the number of moles of each reactant. The reaction quotient is the chemical activity of products (C, D) raised to the number of moles of that product (c, d), divided by the activity of reactants (A, B) raised to the number of moles of that reactant (a, b). R is the gas constant which equals 0.008314 kJ mol^{-1} K, and T is the absolute temperature in Kelvin (297.15 K). The chemical activity values used in the calculations are an approximation based on conditions typically found in soils, $\{NH_4^+\} = 0.0002$; $\{Fe(OH)_3\}$ = 1; $\{NO_2^-\}=0.00001$; $\{Fe^{2+}\} = 10^{-12}$, at a pH of 5. An activity of 1 was used for the solid-phase hydrous Fe(III) oxide minerals, $Fe(OH)_3$, and water (activities of pure solids and liquids are assumed to be equal to unity[39]. Aqueous Fe(III) was not considered as an oxidant in Feammox reactions given that dissolved Fe is not present due to low solubility at a pH of 5 and above[39]. We also do not show calculations coupling NH_4^+ oxidation to
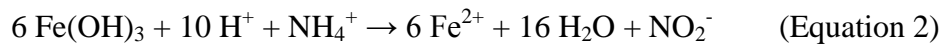
the reduction of goethite (FeOOH), a crystalline Fe oxide. Luther and colleagues[13] reported calculations showing that Feammox to NO_3^- coupled to goethite reduction is not thermodynamically favorable and that Feammox to N_2 coupled to goethite reduction is thermodynamically favorable only below pH 6.8. Free energies of formation were obtained from Stumm and Morgan[40]: NH_4^+, $\bar{G}_f^0$ = -79.37 kJ mol^{-1} ; Fe(OH)$_3$, $\bar{G}_f^0$ = -699 kJ mol^{-1}; Fe^{2+}, $\bar{G}_f^0$ = -78.87 kJ mol^{-1}; and N_2, $\bar{G}_f^0$ = 0 kJ mol^{-1}; NO_2^-, $\bar{G}_f^0$ = -37.2 kJ mol^{-1}; or NO_3^-, $\bar{G}_f^0$ = -111.3 kJ mol^{-1}.

$$3\ \text{Fe(OH)}_3 + 5\ \text{H}^+ + \text{NH}_4^+ \rightarrow 3\ \text{Fe}^{2+} + 9\ \text{H}_2\text{O} + 0.5\ \text{N}_2 \qquad \text{(Equation 1)}$$

$$\Delta G_r = \left[3\Delta G^{\circ}_{f_{Fe^{2+}}} + 9\Delta G^{\circ}_{f_{H_2O}} + 0.5\Delta G^{\circ}_{f_{N_2}} - 3\Delta G^{\circ}_{f_{Fe(OH)_3}} - 5\Delta G^{\circ}_{f_{H^+}} - 1\Delta G^{\circ}_{f_{NH_4^+}} \right]$$
$$+ (0.008314\ \text{kJ mol}^{-1}\ \text{K})(297.15K) \ln \frac{\{10^{-12}\}^3\ \{1\}^9\{0.001\}^{0.5}}{\{1\}^3\{10^{-5}\}^5\{0.0002\}^1}$$

$$\Delta G_r = [3(-78.87) + 9(-237.18) + 0.5(0) - 3(-699) - 5(0) - 1(-79.37)]$$
$$+ (0.008314\ \text{kJ mol}^{-1}\ \text{K})(297.15\ \text{K}) \ln \frac{\{10^{-12}\}^3\ \{1\}^9\{0.001\}^{0.5}}{\{1\}^3\{10^{-5}\}^5\{0.0002\}^1}$$
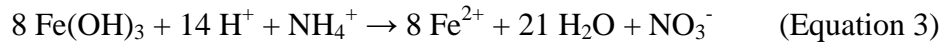
$$\Delta G_r = -244.93\ kJ\ mol^{-1}$$

$$6\ \text{Fe(OH)}_3 + 10\ \text{H}^+ + \text{NH}_4^+ \rightarrow 6\ \text{Fe}^{2+} + 16\ \text{H}_2\text{O} + \text{NO}_2^- \qquad \text{(Equation 2)}$$

$$\Delta G_r = \left[6\Delta G^{\circ}_{f_{Fe^{2+}}} + 16\Delta G^{\circ}_{f_{H_2O}} + 1\Delta G^{\circ}_{f_{NO_2^-}} - 6\Delta G^{\circ}_{f_{Fe(OH)_3}} - 10\Delta G^{\circ}_{f_{H^+}} - 1\Delta G^{\circ}_{f_{NH_4^+}} \right]$$
$$+ (0.008314\ \text{kJ mol}^{-1}\ \text{K})(297.15\ \text{K}) \ln \frac{\{10^{-12}\}^6\ \{1\}^{16}\{0.00001\}^1}{\{1\}^6\{10^{-5}\}^{10}\{0.0002\}^1}$$

$$\Delta G_r = [6(-78.87) + 16(-237.18) + 1(-37.2) - 6(-699) - 10(0) - 1(-79.37)]$$
$$+ (0.008314\,kJ\,mol^{-1}\,K)(297.15\,K)\ln\frac{\{10^{-12}\}^6\,\{1\}^{16}\{0.00001\}^1}{\{1\}^6\{10^{-5}\}^{10}\{0.0002\}^1}$$

$$\Delta G_r = -164.48\,kJ\,mol^{-1}$$

$$8\,Fe(OH)_3 + 14\,H^+ + NH_4^+ \rightarrow 8\,Fe^{2+} + 21\,H_2O + NO_3^- \qquad \text{(Equation 3)}$$

$$\Delta G_r = \left[8\Delta G^\circ_{f_{Fe^{2+}}} + 21\Delta G^\circ_{f_{H_2O}} + 1\Delta G^\circ_{f_{NO_3^-}} - 8\Delta G^\circ_{f_{Fe(OH)_3}} - 14\Delta G^\circ_{f_{H^+}} - 1\Delta G^\circ_{f_{NH_4^+}}\right]$$
$$+ (0.008314\,kJ\,mol^{-1}\,K)(297.15\,K)\ln\frac{\{10^{-12}\}^8\,\{1\}^{21}\{0.00001\}^1}{\{1\}^8\{10^{-5}\}^{14}\{0.0002\}^1}$$

$$\Delta G_r = [8(-78.7) + 21(-237.18) + 1(-111.3) - 8(-699) - 14(0) - 1(-79.37)]$$
$$+ (0.008314\,kJ\,mol^{-1}\,K)(297.15\,K)\ln\frac{\{10^{-12}\}^8\,\{1\}^{21}\{0.00001\}^1}{\{1\}^8\{10^{-5}\}^{14}\{0.0002\}^1}$$

$$\Delta G_r = -206.97\,kJ\,mol^{-1}$$

4. Supplementary References

28. Soil Survey Staff, "Order 1 Soil Survey of the Luquillo Long-Term Ecological Research Grid, Puerto Rico" (U.S. Department of Agriculture Natural Resources Conservation Service, Washington, DC, 1995).

29. Brown, S. Lugo, A.E., Silander, S. & Liegal, L. Research history and opportunities in the Luquillo Experimental Forest. USDA Forest Service General Technical Report **44**, 1-128 (1983).

30. Weaver, P.L. & Murphy, P.G. Forest structure and productivity in Puerto Rico's Luquillo Mountains. *Biotropica* **22**, 69-82 (1990).

31. Hungate, R.E. A roll tube method for cultivation of strict anaerobes. *Methods Microbiol.* 3B, 117-132 (1969).

32. Lovley, D.R. & Phillips, E.J.P. Organic matter mineralization with reduction of ferric iron in anaerobic sediments. *Appl. Environ. Microbiol.* **51**, 683-689 (1986).

33. Silver, W., Scatena, F., Johnson, A., Siccama, T. & Sanchez, M. Nutrient availability in a montane wet tropical forest - spatial patterns and methodological considerations. *Plant Soil* **164**, 129-145 (1994).

34. Malone, J.P., Stevens, R.J. & Laughlin, R.J. Combining the ^{15}N and acetylene inhibition techniques to examine the effect of acetylene on denitrification. *Soil Biol. Biochem.* **30**, 31-37 (1998).

35. Peretyazhko, T. & G. Sposito, G. Iron(III) reduction and phosphorus solubilization in humid tropical forest soils. *Geochimica et Cosmochimica Acta* **69**, 3643-3652 (2005).

36. Chacon, N., Silver, W.L., Dubinsky, E.A. & Cusack, D.F. Iron reduction and soil phosphorus solubilization in humid tropical forests soils: The roles of labile carbon pools and an electron shuttle compound. *Biogeochemistry* **78**, 67-84 (2006).

37. Thompson, A., Chadwick, O.A., Rancourt, D.G. & Chorover, J. Iron-oxide crystallinity increases during soil redox oscillations. *Geochimica et Cosmochimica Acta* **70**, 1710-1727 (2006).

38. Teh, Y.A., Dubinsky, E.A., Silver, W.L. & Carlson, C.M. Suppression of

methanogenesis by dissimilatory Fe(III) reducing bacteria in tropical rain forest soils: implications for ecosystem methane flux. *Global Change Biology* **14**, 413-422 (2008).

39. Langmuir, D. *Aqueous Environmental Geochemistry* 600 (Prentice-Hall, Upper Saddle River, New Jersey, 1997).

40. Stumm, W. & Morgan, J.J. *Aquatic Chemistry: Chemical Equilibria and Rates in Natural Waters* (John Wiley, New York, 1996).